Inorganic Chemistry

Article

pubs.acs.org/IC

Heterolytic Activation of Dihydrogen Molecule by Hydroxo-/Sulfido-Bridged Ruthenium−Germanium Dinuclear Complex. Theoretical Insights

Noriaki Ochi,[†,⊥] Tsuyoshi Matsumoto,[‡] Takeya Dei,[†] Yoshihide Nakao,[†,∥] Hirofumi Sato,[†] Kazuyuki Tatsumi,*[,¶] and Shigeyoshi Sakaki*[,§]

[†]Department of Molecular Engineering, Graduate School of Engineering, Kyoto University, Nishikyo-ku, Kyoto 610-8510, Japan

[‡]Institute of Transformative Bio-Molecules (WPI-ITbM), Nagoya University, Furo-cho, Chikusa-ku, Nagoya 464-8601, Japan

[¶]Research Center for Materials Science, Nagoya University, Furo-cho, Chikusa-ku, Nagoya 464-8602, Japan

[§]Fukui Institute for Fundamental Chemistry, Kyoto University, Takano-Nishihiraki-cho 34-4, Sakyou-ku, Kyoto 606-8103, Japan

Supporting Information

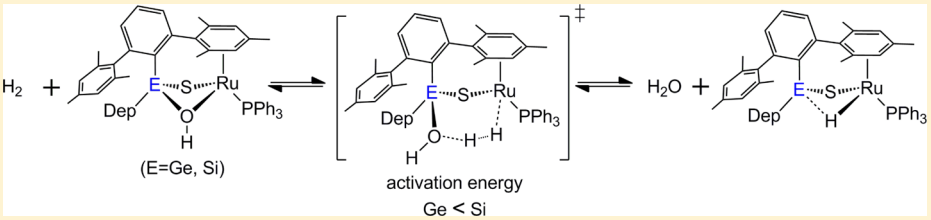

ABSTRACT: Heterolytic activation of dihydrogen molecule (H_2) by hydroxo-/sulfido-bridged ruthenium−germanium dinuclear complex $[Dmp(Dep)Ge(\mu\text{-}S)(\mu\text{-}OH)Ru(PPh_3)]^+$ (**1**) (Dmp = 2,6-dimesitylphenyl, Dep = 2,6-diethylphenyl) is theoretically investigated with the ONIOM(DFT:MM) method. H_2 approaches **1** to afford an intermediate $[Dmp(Dep)(HO)Ge(\mu\text{-}S)Ru(PPh_3)]^+\text{-}(H_2)$ (**2**). In **2**, the Ru−OH coordinate bond is broken but H_2 does not yet coordinate with the Ru center. Then, the H_2 further approaches the Ru center through a transition state $\mathbf{TS_{2-3}}$ to afford a dihydrogen σ-complex $[Dmp(Dep)(HO)Ge(\mu\text{-}S)Ru(\eta^2\text{-}H_2)(PPh_3)]^+$ (**3**). Starting from **3**, the H−H σ-bond is cleaved by the Ru and Ge−OH moieties to form $[Dmp(Dep)(H_2O)Ge(\mu\text{-}S)Ru(H)(PPh_3)]^+$ (**4**). In **4**, hydride and H_2O coordinate with the Ru and Ge centers, respectively. Electron population changes clearly indicate that this H−H σ-bond cleavage occurs in a heterolytic manner like H_2 activation by hydrogenase. Finally, the H_2O dissociates from the Ge center to afford $[Dmp(Dep)Ge(\mu\text{-}S)Ru(H)(PPh_3)]^+$ (**PRD**). This step is rate-determining. The activation energy of the backward reaction is moderately smaller than that of the forward reaction, which is consistent with the experimental result that **PRD** reacts with H_2O to form **1** and H_2. In the Si analogue $[Dmp(Dep)Si(\mu\text{-}S)(\mu\text{-}OH)Ru(PPh_3)]^+$ ($\mathbf{1_{Si}}$), the isomerization of $\mathbf{1_{Si}}$ to $\mathbf{2_{Si}}$ easily occurs with a small activation energy, while the dissociation of H_2O from the Si center needs a considerably large activation energy. Based on these computational findings, it is emphasized that the reaction of **1** resembles well that of hydrogenase and the use of Ge in **1** is crucial for this heterolytic H−H σ-bond activation.

INTRODUCTION

Heterolytic H−H σ-bond activation of dihydrogen molecule (H_2) with transition metal complex is one of the most important research subjects in biochemistry and inorganic chemistry,[1] because the heterolytic activation of H_2 is involved as a key step in hydrogen metabolism by hydrogenases.[2] The hydrogenases are classified into three categories from the viewpoint of a metal center in an active site: (1) hydrogenase containing an iron−iron cluster, which is named [FeFe],[3,4] (2) hydrogenase containing an nickel−iron cluster, which is named [NiFe],[5−7] and (3) hydrogenase containing only one iron center, which is named [Fe].[8−10] Among them, [NiFe]-hydrogenases have been widely investigated. To explore and mimic its catalysis, many experiments have been carried out to synthesize good models of [NiFe]-hydrogenase,[2i,11] and the activation reactions of H_2 with such hydrogenase models as Ir−Ir,[12,13] Rh−Rh,[14] Mo−Mo,[15] W−Ir,[16] W−Ru,[17], Ru−Ni,[18] and Fe−Ni[19] dinuclear complexes have been reported.

Recently, Matsumoto, Tatsumi, and their co-workers synthesized a hydroxo-/sulfido-bridged Ru−Ge dinuclear complex $[Dmp(Dep)Ge(\mu\text{-}S)(\mu\text{-}OH)Ru(PPh_3)]^+(BAr^F{}_4)^-$ (Dmp = 2,6-dimesitylphenyl, Dep = 2,6-diethylphenyl, $Ar^F{}_4$ = 3,5-$(CF_3)_2C_6H_3$) and reported its interesting reactions,[20] as follows: (1) This complex performs σ-bond activation of H_2 at room temperature to afford H_2O and $[Dmp(Dep)Ge(\mu\text{-}S)Ru(H)(PPh_3)]^+(BAr^F{}_4)^-$, which is similar to the activation reaction of H_2 by hydrogenase, and (2) addition of H_2O to the product induces the reverse reaction to afford H_2 and the original Ru−Ge complex, indicating that the reversible reaction

Received: October 9, 2014
Published: January 5, 2015

DOI: 10.1021/ic502463y
Inorg. Chem. 2015, 54, 576−585

is successfully performed by this Ru−Ge complex, as shown in Scheme 1. Although many σ-bond activation reactions of H_2

Scheme 1

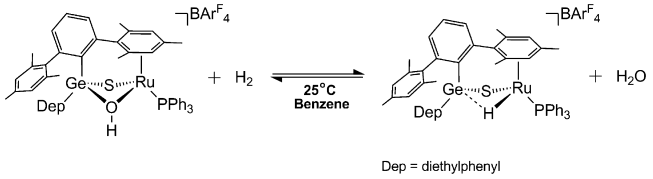

have been reported, this type of reversible reaction has not been reported yet, to our knowledge. This reversible reaction is of considerable interest from both viewpoints of a model reaction of hydrogenase and one kind of dihydrogen storage reaction; note that the chemical reaction for the formation of dihydrogen molecule from water is very attractive. Also, this complex consisting of a sulfide-bridged transition-metal and heavy main-group elements is a new type of complex. The Goldberg group reported similar H_2 activation with palladium(II) hydroxide and methoxide complexes to afford water and alcohol, respectively.[21] Though these reactions are very interesting, the mononuclear complexes were employed in their work. Hence, it is interesting to clarify whether the heavy main-group element plays crucial roles in the σ-bond activation reaction or not.

The H_2 activation with dinuclear complexes has been theoretically investigated by several groups. Hoffmann and Trinquier previously investigated the activation of H_2 by a dinuclear manganese complex $[Mn_2(CO)_6]$ with an extended Hückel MO method and reported that this reaction occurs through a four-center transition state.[22a] Ienco, Mealli, and co-workers investigated the activation of H_2 by a sulfido-bridged rhodium dinuclear complex $[(H_3P)_3Rh(\mu\text{-}S)_2Rh(PH_3)_3]$ with the DFT method and reported that the Ru-(μ-S) moiety participates in heterolytic activation of H_2.[22b] Nocera et al. investigated the activation reaction of H_2 by an iridium dinuclear complex with the DFT method and disclosed that two Ir centers cooperatively play important roles in the reaction.[23]

In the above-mentioned H−H σ-bond activation reaction by $[Dmp(Dep)Ge(\mu\text{-}S)(\mu\text{-}OH)Ru(PPh_3)]^+(BAr^F_4)^-$, we found new important questions: It is not clear which of the μ-S and μ-OH groups participates in the reaction, because both the μ-S and μ-OH groups are considered to be reactive for the H−H σ-bond activation reaction. Also, it is not clear what roles the germanium element plays in the reaction. If the role of the germanium is different from that of the sulfur in the σ-bond activation which has been reported by Mealli et al.,[22b] it is of considerable interest because such knowledge provides us with a new possibility to employ various elements in σ-bond activation reactions.

In this theoretical work, we investigated the H−H σ-bond activation of H_2 to afford H_2O promoted by the hydroxo-/sulfido-bridged Ru−Ge dinuclear complex $[Dmp(Dep)Ge(\mu\text{-}S)(\mu\text{-}OH)Ru(PPh_3)]^+$ (**1**). Our purposes here are to clarify the mechanism of this interconversion reaction, in particular, how the H−H σ-bond is cleaved by **1**, to disclose which of the μ-S and μ-OH groups participates in the σ-bond activation reaction, to understand what roles the ruthenium and germanium elements play in this reaction, and to make a comparison of the reactivity between **1** and the silicon analogue.

COMPUTATIONAL DETAILS

Geometries were optimized with the ONIOM method,[24] where the DFT method with the B3LYP functional[25] was used for an important moiety and the MM method with the UFF force field was employed for a whole system. One mesityl group of the Dmp coordinates with the Ru center, but another is free; see Scheme 1. In the important moiety which was calculated with the DFT method, H atoms were substituted for three methyl groups of the mesityl group coordinating with the Ru center, another free mesityl group, three phenyl groups of triphenylphosphine, and the Dep group bound with the Ge center. We ascertained that each equilibrium structure exhibited no imaginary frequency and each transition state exhibited one imaginary frequency. The solvation effects of benzene were evaluated with the PCM method.[26] Two kinds of basis set systems were used. The smaller system (BS1) was used for geometry optimization. In this BS1, core electrons of Ru (up to 3f) were replaced with effective core potentials (ECPs)[27] and its valence electrons were represented with a (311111/22111/411) basis set.[27] For H, C, O, Si, P, S, and Ge, 6-31G(d) basis sets were employed.[28] The better basis set system (BS2) was used for evaluation of energy change. In this BS2, a (311111/22111/411/11) basis set[27,29] was employed for Ru, where the same ECPs[27] as those of BS1 were employed for core electrons. For H, C, N, O, Si, P, S, and Ge, the 6-311G(d) basis sets[30] were employed. In both BS1 and BS2, a p-polarization function[31] was added to the H atoms of the dihydrogen molecule, μ-OH, and H_2O. The zero-point energy was evaluated with the ONIOM(B3LYP/BS1:UFF) method under assumption of harmonic oscillator. The potential energy change (ΔE) with zero-point energy correction and the Gibbs energy ($\Delta G°$) in solution were employed for discussion, where the translational entropy was evaluated with the method developed by Whitesides et al.[32] as in our previous works.[33]

The Gaussian 09 program package[34] was used for all calculations. Population analysis was carried out with the method of Weinhold et al.[35]

RESULTS AND DISCUSSION

Coordination of Dihydrogen Molecule (H_2). As shown in Scheme 2, four kinds of approaching course of H_2 to the Ru center are possible. In path 1O, H_2 approaches the Ru center on the μ-OH side of **1**, and in path 1S, it approaches the Ru

Scheme 2[a]

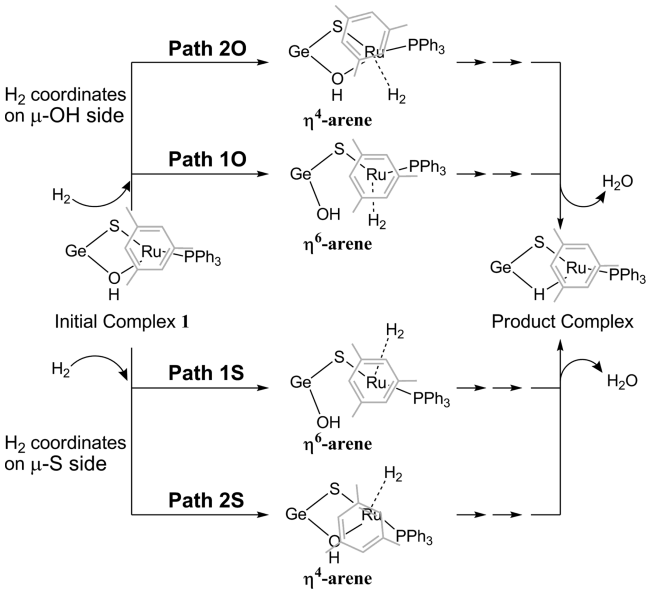

[a]Arene group drawn by gray indicates arene group coordinated to Ru center.

DOI: 10.1021/ic502463y
Inorg. Chem. 2015, 54, 576−585

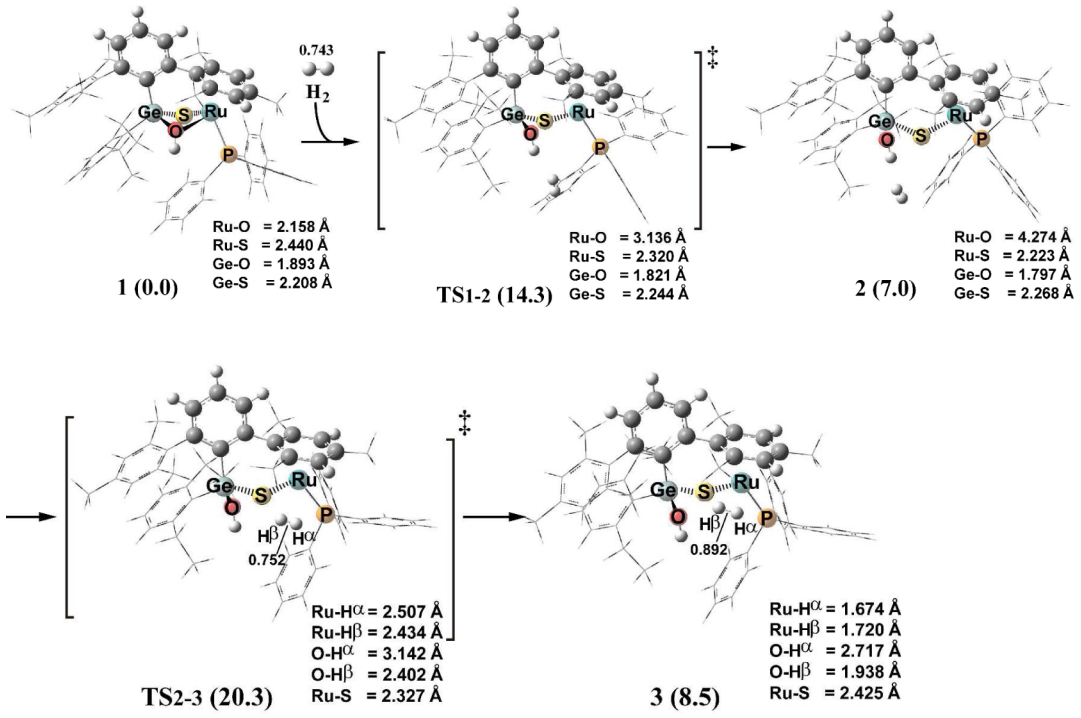

Figure 1. Geometry changes in H_2 coordination to $[Dmp(Dep)Ge(\mu\text{-}OH)(\mu\text{-}S)Ru(PPh_3)]^+$ (**1**) through path 1O. Bond lengths are in angstroms. In parentheses is the relative energy (in kcal/mol) to **1** + H_2, where the ONIOM(B3LYP/BS2:UFF) method was employed and the solvation effect was evaluated with the PCM method.

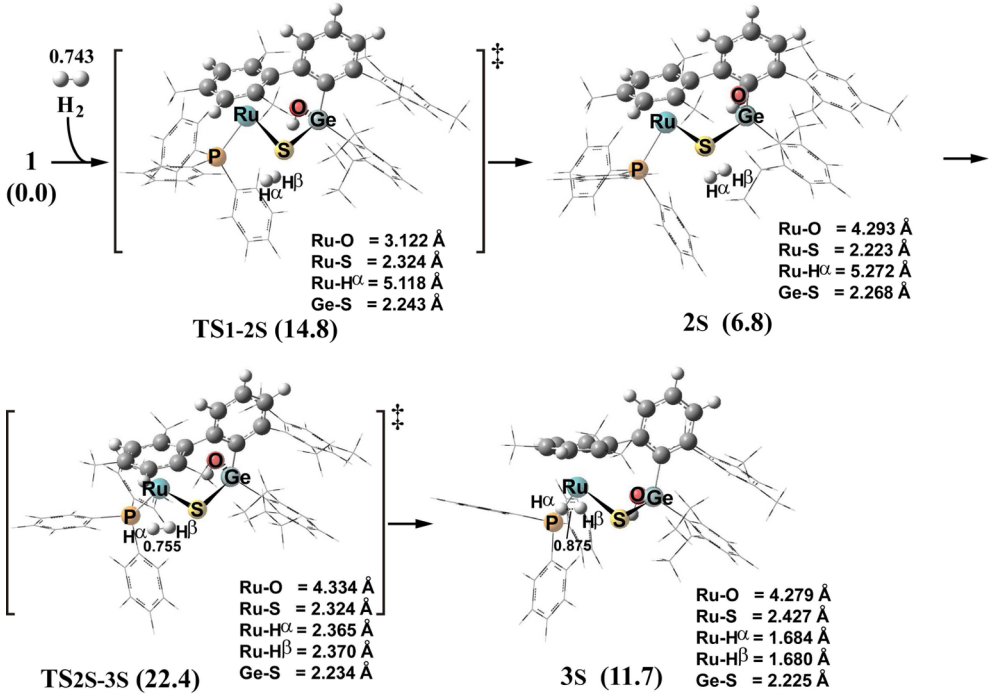

Figure 2. Geometry changes in H_2 coordination to $[Dmp(Dep)Ge(\mu\text{-}OH)(\mu\text{-}S)Ru(PPh_3)]^+$ (**1**) through path 1S. Bond lengths are in angstroms. In parentheses is the relative energy (in kcal/mol) to **1** + H_2, by the ONIOM(B3LYP/BS2:UFF) method, where the solvation effect was evaluated with the PCM method.

center on the μ-S side. In both paths, the OH group on the Ge dissociates from the Ru center but the arene moiety keeps an η^6-coordination structure. In paths 2O and 2S, H_2 approaches the Ru center on the μ-OH and μ-S sides, respectively, where the OH group keeps the coordinate bond with the Ru center but the η^6-coordination structure of the arene moiety changes to an η^4-coordination one; remember that the arene can take the η^4-coodination structure in several cases. We investigated all these reaction courses and found that paths 2S and 2O are very unfavorable, probably because the η^4-coordination structure of the arene is much less stable than the η^6-coordination one.

DOI: 10.1021/ic502463y
Inorg. Chem. 2015, 54, 576−585

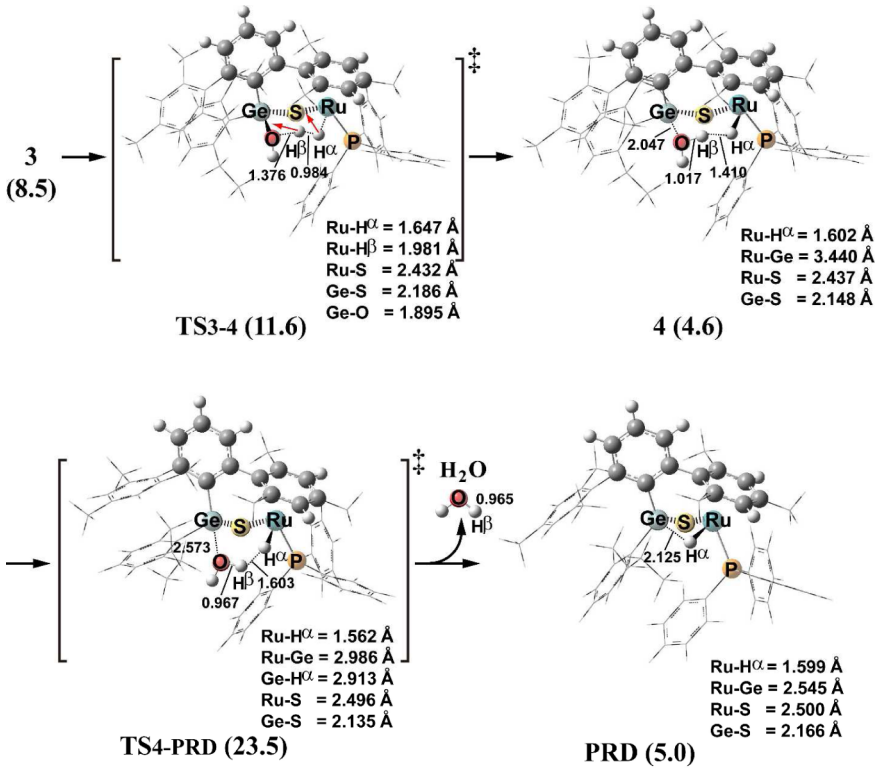

Figure 3. Geometry changes in H−H σ-bond activation and H_2O dissociation with $[Dmp(Dep)Ge(\mu\text{-}OH)(\mu\text{-}S)Ru(PPh_3)]^+$ (**1**) through path 1O. Bond lengths are in angstroms. In parentheses is the relative energy (in kcal/mol) to **1** + H_2, by the ONIOM(B3LYP/BS2:UFF) method, where the solvation effect was evaluated with the PCM method. Arrows in $\mathbf{TS_{3-4}}$ repesent important movements of nuclei in the imaginary frequency.

Here, we wish to focus on paths 1S and 1O; see Figure S1 and S2 for geometry changes in paths 2S and 2O.

In path 1O, the Ru−O distance becomes longer as H_2 approaches the Ru center, to afford an intermediate $[Dmp(Dep)(HO\text{-}Ge)(\mu\text{-}S)Ru(PPh_3)]^+\text{-}(H_2)$ (**2**) through a transition state $\mathbf{TS_{1-2}}$; see Figure 1. In $\mathbf{TS_{1-2}}$, the Ru−O distance becomes considerably longer by 0.978 Å and the Ru−S distance becomes somewhat shorter by 0.120 Å. In **2**, the Ru−O distance (4.274 Å) is very long, indicating that the μ-OH group completely dissociates from the Ru center and it is bound only with the Ge atom. It is noted that the Ru−S distance becomes considerably shorter, 2.223 Å, which will be discussed below in more detail. In both **2** and $\mathbf{TS_{1-2}}$, the H_2 molecule is very distant from the Ru center. These geometrical features suggest that $\mathbf{TS_{1-2}}$ is not a transition state for H_2 coordination with the Ru center and **2** is not a dihydrogen σ-complex; in other words, **2** is understood to be an isomer of **1** in which the OH group dissociates from the Ru center and $\mathbf{TS_{1-2}}$ is a transition state for the isomerization of **1** to **2**. The H_2 further approaches the Ru center through a transition state $\mathbf{TS_{2-3}}$ to afford a dihydrogen σ-complex $[Dmp(Dep)(HO\text{-}Ge)(\mu\text{-}S)Ru(\eta^2\text{-}H_2)(PPh_3)]^+$ (**3**). In $\mathbf{TS_{2-3}}$, the Ru−H^α and Ru−H^β distances are about 2.5 Å, the O−H^α and O−H^β distances are very long, and the H^α−H^β distance (0.752 Å) is moderately longer than in a free H_2 molecule. In **3**, the Ru−H^α and Ru−H^β distances are 1.674 and 1.720 Å, respectively, and the H^α−H^β bond becomes longer than in a free H_2 molecule by 0.149 Å. These are typical geometrical features of the dihydrogen σ-complex. Hence, this $\mathbf{TS_{2-3}}$ is a transition state for the H_2 coordination. The Ru−S distance considerably increases to 2.425 Å in **3**, which is close to that of **1**.[36] This is because the Ru−S interaction becomes weak by the coordination of the H_2 molecule. The O−H^β distance (1.938 Å) is not very long, indicating that the approach of H^β to O is already prepared in **3**.

In the path 1S, H_2 approaches the Ru center on the μ-S side to afford an intermediate $\mathbf{2_S}$ through a transition state $\mathbf{TS_{1-2S}}$, as shown in Figure 2. This reaction course was investigated to examine if the μ-S atom participates in the H−H σ-bond activation reaction. In $\mathbf{TS_{1-2S}}$, the Ru−O distance becomes considerably elongated to 3.122 Å, while the Ru−S distance changes little and the Ru−H_2 distance is still very long. These geometrical features indicate that $\mathbf{2_S}$ is not a dihydrogen σ-complex but an isomer of **1** like **2**. Then, the H_2 coordinates with the Ru center through a transition state $\mathbf{TS_{2S\text{-}3S}}$ to form a dihydrogen σ-complex $\mathbf{3_S}$. These geometry changes are similar to those in the path 1O. In $\mathbf{TS_{2S\text{-}3S}}$, the Ru−$H^\alpha$ and Ru−H^β distances decrease to 2.365 and 2.370 Å, respectively. In $\mathbf{3_S}$, the Ru−H^α and Ru−H^β distances are 1.684 and 1.680 Å, respectively, and the H^α−H^β distance increases to 0.875 Å. These features are consistent with our understanding that $\mathbf{3_s}$ is a typical dihydrogen σ-complex.

Geometry Changes in H−H σ-bond Activation and H_2O Dissociation. Starting from **3**, the H−H σ-bond activaion occurs through a transition state $\mathbf{TS_{3-4}}$ to afford a ruthenium(II) hydride water complex $[Dmp(Dep)(H_2O\text{-}Ge)(\mu\text{-}S)Ru(H)(PPh_3)]^+$ (**4**), as shown in Figure 3. In $\mathbf{TS_{3-4}}$, the H^α−H^β distance considerably increases to 0.984 Å and the O−H^β distance considerably decreases to 1.376 Å, indicating that the H^β is moving from the H^α toward the OH group. Consistent with these geometry changes, the imaginary frequency mainly involves the position change of the H^β toward the OH group; see the arrows in $\mathbf{TS_{3-4}}$ (in Figure 3) which represent important movements of nuclei in the imaginary frequency. In **4**, the O−H^β distance (1.017 Å) is almost the same as that of

DOI: 10.1021/ic502463y
Inorg. Chem. 2015, 54, 576−585

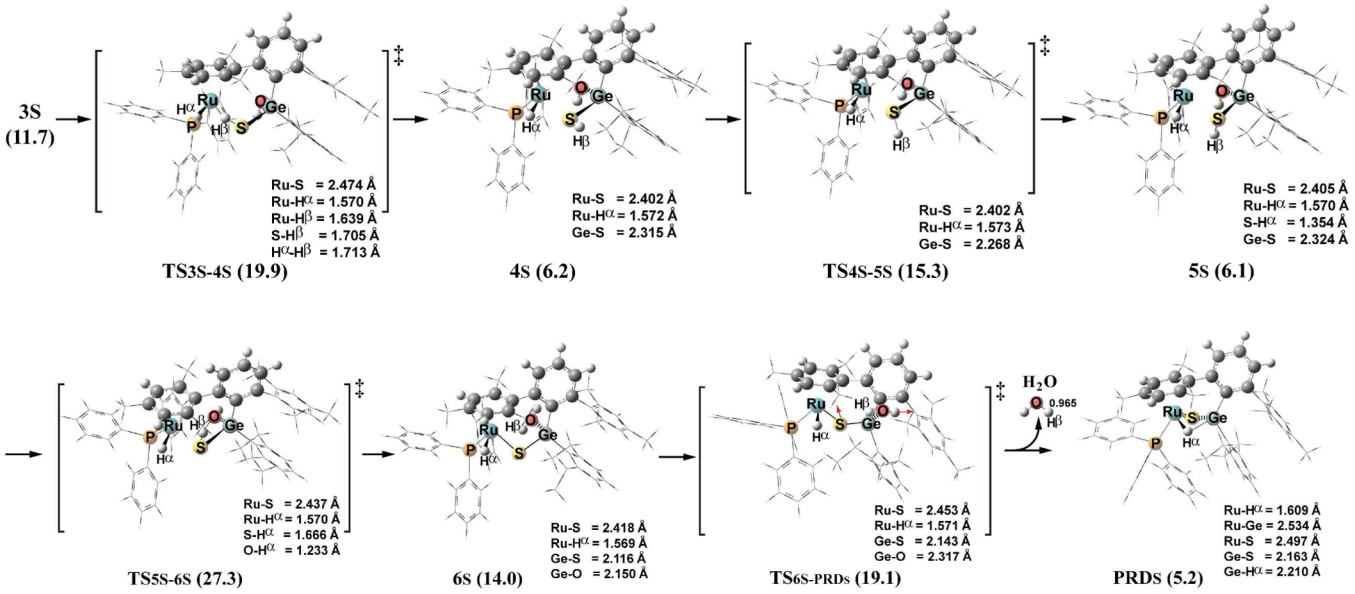

Figure 4. Geometry changes in H−H σ-bond activation and H_2O dissociation with $[Dmp(Dep)Ge(\mu\text{-}OH)(\mu\text{-}S)Ru(PPh_3)]^+$ (**1**) on the μ-S side through path 1S. In parentheses is the relative energy (in kcal/mol) to **1** + H_2, by the ONIOM(B3LYP/BS2:UFF) method, where the solvation effect was evaluated with the PCM method. Red arrows in $\mathbf{TS_{6S\text{-}PRDs}}$ represent important movements of nuclei in the imaginary frequency. Bond lengths are in angstroms.

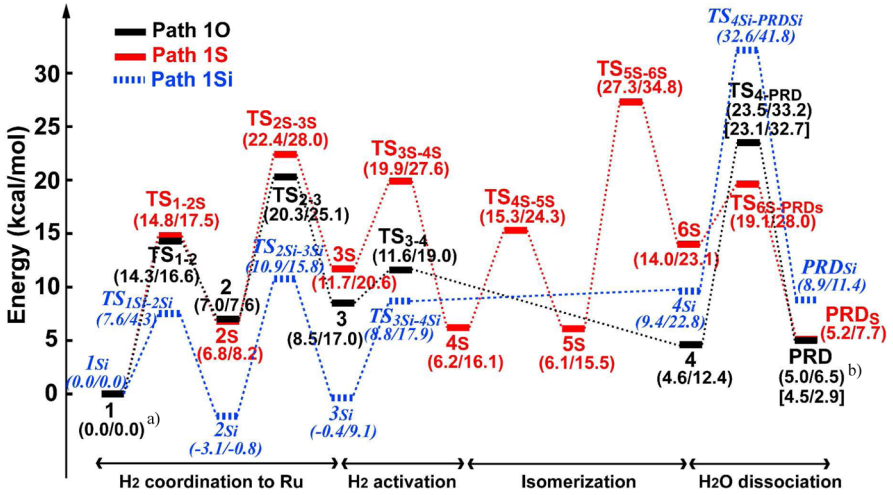

Figure 5. Energy changes[a] in paths 1O, 1S, and 1Si. Black, red, and blue lines indicate energy changes in paths 1O, 1S, and 1Si, respectively. [a]In parentheses, the potential energy with zero-point energy correction and the Gibbs energy change (kcal/mol) are presented before and after the slash, respectively. The ONIOM(B3LYP/BS2:UFF) method was employed with the PCM method. The potential energy changes are plotted here. [b]The M06-calculated values are presented in the brackets.

water, clearly indicating that water molecule is formed. Because of the formation of water, the Ge−O distance becomes considerably long. However, it is still 2.047 Å, indicating the presence of the coordinate bond between the water and the Ge center. It is noted that the H^{α}−H^{β} distance (1.410 Å) is not very long even in **4**, suggesting that some attractive interaction such as electrostatic interaction exists between them. This type of a rather short H−H distance is often observed in the product of the H−H heterolytic activation reaction.[37] Then, the H_2O dissociates from the Ge center through a transition state $\mathbf{TS_{4\text{-}PRD}}$ to afford a final product, $[Dmp(Dep)Ge(\mu\text{-}S)Ru(H)(PPh_3)]^+$ (**PRD**) and H_2O. In $\mathbf{TS_{4\text{-}PRD}}$, the Ge−O distance increases to 2.573 Å. In **PRD**, the Ru−H^{α} bond distance decreases to 1.599 Å, indicating that the Ru−H(hydride) bond is completely formed. It is noted here that the Ge−H^{α} distance is 2.125 Å. A similar Ge−H^{α} distance is often observed in the transition-metal germane σ-complex,[38] suggesting that the Ru−H^{α} bond interacts with the Ge center to contribute to the stabilization of **PRD**.

In path 1S starting from the other intermediate $\mathbf{3_S}$, the H−H σ-bond cleavage occurs through a transition state $\mathbf{TS_{3S\text{-}4S}}$ to afford an intermediate $[Dmp(Dep)Ge(\mu\text{-}OH)(\mu\text{-}SH^{\beta})Ru(H^{\alpha})(PPh_3)]^+$ ($\mathbf{4_S}$), as shown in Figure 4. In $\mathbf{TS_{3S\text{-}4S}}$, the H^{α}−H^{β} distance becomes considerably longer, 1.713 Å, indicating that the H^{α}−H^{β} σ-bond is almost broken. The Ru−H^{α} and S−H^{β} distances are 1.570 and 1.705 Å, respectively, indicating that the Ru−H^{α}(hydride) and S−H^{β} bonds are almost formed. As expected above, the μ-S atom participates in the H−H σ-bond activation in this reaction course. In $\mathbf{4_S}$, the H^{β} is bound with the μ-S, but the Ru−S distance becomes moderately shorter in

DOI: 10.1021/ic502463y
Inorg. Chem. 2015, 54, 576−585

$\mathbf{4_S}$ than in $\mathbf{3_S}$, indicating that the SH group plays the role of a bridging ligand between the Ru and Ge centers. The intermediate $\mathbf{4_S}$ isomerizes to [Dmp(Dep)Ge(μ-OH)Ru(μ-SH$^{\beta}$)(H$^{\alpha}$)(PPh$_3$)]$^+$ ($\mathbf{5_S}$) through a transition state $\mathbf{TS_{4S\text{-}5S}}$, where the H$^{\beta}$ atom is changing its position by the rotation of the SH group around the Ge−S bond. In $\mathbf{5_S}$, the H$^{\beta}$ takes the position close to the OH group. When going from $\mathbf{5_S}$ to $\mathbf{6_S}$, the rotation further continues to bring the H$^{\beta}$ atom toward the OH group and the H$^{\beta}$ simultaneously migrates from the S atom to the OH group through a transition state $\mathbf{TS_{5S\text{-}6S}}$ to afford a ruthenium(II) hydride water complex [Dmp(Dep)(H$_2$O-Ge)(μ-S)Ru(H)(PPh$_3$)]$^+$ ($\mathbf{6_S}$). In $\mathbf{TS_{5S\text{-}6S}}$, the S−H$^{\beta}$ distance is increasing and the O−H$^{\beta}$ distance is decreasing. In $\mathbf{6_S}$, the Ge−O distance (2.150 Å) is considerably long and the O−H$^{\beta}$ distance is almost the same as that of water, indicating that water is completely formed and interacts with the Ge center as in **6**. The H$_2$O dissociates from the Ge center through a transition state $\mathbf{TS_{6S\text{-}PRDs}}$ to afford a final product, [Dmp-(Dep)Ge(μ-S)Ru(H)(PPh$_3$)]$^+$ (**PRDs**) and H$_2$O. In $\mathbf{TS_{6S\text{-}PRDs}}$, the S atom moves from the position cis to the H$^{\alpha}$ atom to the position trans to the H$^{\alpha}$ concomitantly with the increase in the Ge−OH$_2$ distance. **PRDs** is an isomer of **PRD**, which is the product in path 1O; note that the positions of the H$^{\alpha}$ and S atoms are different between **PRD** and **PRDs**, though the difference is not essential; actually, **PRD** is as stable as **PRDs**, as shown in Figure 5.

Energy Changes in the Conversion of H_2 to H_2O. We calculated energy changes by the H$_2$ coordination step in paths 1O and 1S with the ONIOM(B3LYP/BS2:UFF) method, where solvation effects of benzene were evaluated with the PCM method.[26] In the path 1O, $\mathbf{TS_{1-2}}$ is more unstable than the sum of reactants, **1** + H$_2$, by 14.3 (16.6) kcal/mol,[39] as shown in Figure 5. The intermediate **2** is 7.0 (7.6) kcal/mol more unstable than the sum of reactants.[40] This is because the Ru−(μ-OH) bond is almost broken in **2** but the H$_2$ molecule does not coordinate with the Ru center; see above. $\mathbf{TS_{2-3}}$ is much more unstable than $\mathbf{TS_{1-2}}$, and also **3** is somewhat more unstable than **2**. This is probably because the H$_2$ coordination induces a larger distortion in the Dep ligand in $\mathbf{TS_{2-3}}$ and **3** than in $\mathbf{TS_{1-2}}$ and **2**, respectively. In path 1S, the E_a and $\Delta G^{\circ\ddagger}$ values for $\mathbf{TS_{1-2S}}$ and $\mathbf{TS_{2S\text{-}3S}}$ are larger than those for $\mathbf{TS_{1-2}}$ and $\mathbf{TS_{2-3}}$ in path 1O. Also, $\mathbf{3_S}$ is somewhat more unstable than **3**.

In path 1O, the H−H σ-bond cleavage occurs through $\mathbf{TS_{3-4}}$ with the activation energy 11.6 (19.0) kcal/mol, as shown in Figure 5. Finally, the H$_2$O dissociates from the Ge center with a somewhat large activation energy of 23.5 (33.2) kcal/mol, which is defined as the energy difference between the transition state and the sum of reactants **1** + H$_2$, because no intermediate is more stable than **1**. This result indicates that the rate-determining step is the H$_2$O dissociation through $\mathbf{TS_{4\text{-}PRD}}$. In path 1S, the activation energy for the H−H cleavage through $\mathbf{TS_{5S\text{-}6S}}$ is 19.9 (27.6) kcal/mol. It is noted that the H−H σ-bond cleavage by the Ru-(μ-S) moiety (path 1S) needs a larger activation energy than that by the Ru and Ge−OH moieties (path 1O). The rate-determining step is the H$_2$O formation through $\mathbf{TS_{5S\text{-}6S}}$, the activation barrier of which is 27.3 (34.8) kcal/mol relative to the reactant **1**. Because the $\Delta G^{\circ\ddagger}$ is moderately larger in path 1S than in path 1O, it is concluded that path 1O is more favorable than path 1S. Hereafter, we wish to discuss path 1O. We reoptimized the important $\mathbf{TS_{4\text{-}PRD}}$ and **PRD** and recalculated the $\Delta G^{\circ\ddagger}$ and ΔG° values with the M06 functional[41] to consider the dispersion correction. Though the $\Delta G^{\circ\ddagger}$ (32.7 kcal/mol) is little different from the ONIOM-calculated value, the ΔG° value becomes somewhat smaller, 2.9 kcal/mol; see Table S9 in the SI for more details.

The reverse reaction of this conversion is experimentally observed by adding excess H$_2$O. Although **PRD** is moderately more unstable than **1** + H$_2$, the energy difference is small between them, as was discussed above; see also Figure 5 and Table S9. Because the most unstable transition state is $\mathbf{TS_{4\text{-}PRD}}$, the rate-determining step in the reverse reaction is the coordination of H$_2$O with the Ge center through $\mathbf{TS_{4\text{-}PRD}}$. The activation energy of this step is calculated to be 18.5 (26.7) kcal/mol with the ONIOM(B3LYP:UFF) and 18.6 (29.8) kcal/mol with the M06 functional. The difference in activation energy between the forward and reverse reactions is small, indicating that the reversible reaction between H$_2$ and H$_2$O is efficiently promoted by **1**. This is consistent with the experimental report.[20]

Electronic Process in the Conversion of H_2 to H_2O. When going to **2** from **1** through $\mathbf{TS_{1-2}}$, the donating μ-OH group dissociates from the Ru center. It is noted that the H$^{\alpha}$ and H$^{\beta}$ atomic populations of H$_2$ change little when going to $\mathbf{TS_{1-2}}$ from **1**, as shown in Figure 6, indicating that the H$_2$ coordination is not involved in this step. The Ru atomic population changes little too, though the μ-OH group dissociates from the Ru center. On the other hand, the S atomic population somewhat decreases. These population changes indicate that the decrease in the Ru atomic population is induced by the dissociation of the donating OH group but the charge transfer (CT) from the μ-S to the Ru becomes stronger in **2** than in **1** to compensate for the decrease in the Ru atomic population. The increase in the μ-S → Ru CT interaction leads to the shortening of the Ru−S distance in **2**. This is consistent with the geometry change that the Ru−S distance decreases when going from **1** to **2**. This decrease in the Ru−S bond distance contributes to the stabilization of **2**. Because the OH group interacts with both the Ru and Ge centers in **1** but only with the Ge center in **2**, the Ge−OH distance becomes shorter in **2** than in **1**, which also contributes to the stabilization of **2**. In other words, the destabilization energy by the Ru−OH bond breaking is somewhat compensated by the strengthening of the Ru−S and Ge−OH bonds. Hence, the isomerization of **1** to **2** is not very difficult.

When going to **3** from **2**, the H$_2$ coordinates with the Ru center. This coordination is moderately endothermic. In this step, the electron population of the H$_2$ moiety considerably decreases and the Ru atomic population considerably increases, indicating that the CT occurs from the H$_2$ to the Ru center.

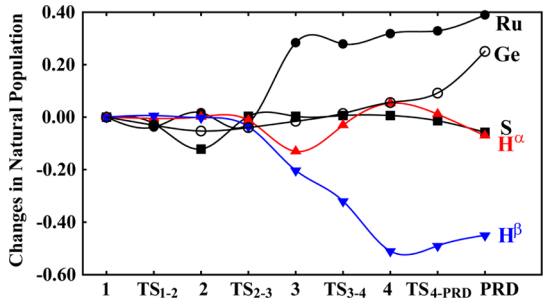

Figure 6. Electron population changes in the conversion of H$_2$ to H$_2$O evaluated with the ONIOM(B3LYP/BS2:UFF). The solvation effects are incorporated with the PCM method.

DOI: 10.1021/ic502463y
Inorg. Chem. 2015, 54, 576−585

Simultaneously, the S atomic population as well as the Ru−S distance returns to almost the same value as that of **1**. These results indicate that the μ-S group stabilizes the coordinatively unsaturated species **2** by the CT from the μ-S to the Ru center in **2** but the CT interaction becomes weak in **3** because the Ru moiety receives some of the electron population from the H_2 molecule in **3**.

Important population changes are observed when going to **4** from **3**, as follows: The H^{α} atomic population considerably increases but the H^{β} atomic population considerably decreases when going to **4** from **3**. These results clearly indicate that this H−H σ-bond cleavage occurs in a heterolytic manner like hydrogenase.[2,42] In other words, **1** works well as a functional model of hydrogenase. Interestingly, the Ru and the O atoms of the Ge−OH moiety cooperatively participate in the H_2 activation, whereas they are separated well from each other by the μ-S ligand; see **3** in Figure 1. This is a new feature in the heterolytic H−H σ-bond activation because an anion X ligand directly coordinating with the metal usually participates in the heterolytic σ-bond activation reactions previously reported.[43,44] These features are similar to the H−H σ-bond activation by a frustrated Lewis pair;[45] actually, several theoretical works reported that the H−H σ-bond is cleaved in a heterolytic manner by the frustrated Lewis pair.[46]

Heterolytic Activation of the H−H σ-bond by a Si Analogue [Dmp(Dep)Si(μ-OH)(μ-S)Ru(PPh_3)]$^+$. As discussed above and shown in Figure 5, the rate-determining step is the H_2O dissociation from the Ge center in the conversion of H_2 to H_2O of path 1O. Hence, it is likely that the Ge plays important roles in this reversible reaction.

To elucidate the reason why the Ge atom is crucial in **1**, we investigated the reaction of H_2 with the Si analogue [Dmp(Dep)Si(μ-OH)(μ-S)Ru(PPh_3)]$^+$ ($\mathbf{1_{Si}}$), in which the Si atom was substituted for the Ge atom. Because the geometry changes are similar to those of the reaction by **1**, we omitted the discussion; see Figure S4 for geometry changes. As shown in Figure 5, the isomerization of $\mathbf{1_{Si}}$ to $\mathbf{2_{Si}}$ occurs through a transition state $\mathbf{TS_{1Si\text{-}2Si}}$ with the activation energy of 7.6 (4.3) kcal/mol, which is much lower than that in the Ge analogue **1**. This is because the dissociation of the OH group from the Ru center leads to the formation of the very strong Si−OH bond, whose bond energy will be discussed below. In the H−H σ-bond cleavage, however, the activation energy relative to $\mathbf{3_{Si}}$ is considerably larger than that of the reaction by **1**; see the energy difference of 9.2 (8.8) kcal/mol between $\mathbf{3_{Si}}$ and $\mathbf{TS_{3Si\text{-}4Si}}$ and that of 3.1 (2.0) kcal/mol between **3** and $\mathbf{TS_{3-4}}$. Also, the H−H σ-bond cleavage step is considerably endothermic in $\mathbf{1_{Si}}$. The H_2O dissociation requires similar activation energy relative to **4**/**4Si**; it is 22.2 (19.0) kcal/mol in the reaction by $\mathbf{1_{Si}}$ and 18.9 (20.8) kcal/mol in the reaction by **1**, as shown in Figure 5. However, $\mathbf{TS_{4Si\text{-}PRDSi}}$ is calculated at a much higher energy than $\mathbf{TS_{4\text{-}PRD}}$. Because the activation energy relative to $\mathbf{4/4_{Si}}$ is similar for the reactions of **1** and $\mathbf{1_{Si}}$, the much more unstable $\mathbf{TS_{4Si\text{-}PRDSi}}$ than $\mathbf{TS_{4\text{-}PRD}}$ arises from the fact that $\mathbf{4_{Si}}$ is much less stable than **4**.

To clarify the reason for this difference, we calculated the Si−OH, Ge−OH, Si−OH_2, and Ge−OH_2 bond energies, because the Ge−OH/Si−OH bond is converted to the Ge−OH_2/Si−OH_2 bond in this process. The Si−OH bond energy (137.2 kcal/mol) is much larger than the Ge−OH one (100.2 kcal/mol) by 37.0 kcal/mol, where $Ph_2E(SH)(OH)$ (E = Si or Ge) was employed as a model, considering the Si and Ge moieties in **1**; see Figure S7 for the geometry. In the evaluation of the Ge−OH_2 and Si−OH_2 bond energies, we must employ a reasonable model, because the Ge/Si center is considered to be cationic in $\mathbf{4/4_{Si}}$. To mimic the Ge and Si moieties in **4** and $\mathbf{4_{Si}}$, model compounds $GePh_2(SH)(H_2O)^+$ ($\mathbf{Ge_M}$) and $SiPh_2(SH)(H_2O)^+$ ($\mathbf{Si_M}$) were employed. The geometries of $\mathbf{Ge_M}$ and $\mathbf{Si_M}$ resemble those of the Ge and Si moieties in **4** and $\mathbf{4_{Si}}$, respectively; see Figure S8. For instance, the sum of the C^1−Ge-C^2, C^1−Ge-S, and C^2−Ge-S angles is 353.5°in $\mathbf{Ge_M}$ and that of the C^1−Si−C^2, C^1−Si−S, and C^2−Si−S angles is 350.4° in $\mathbf{Si_M}$. These values are close to 360°, indicating that the $GePh_2(SH)$ and $SiPh_2(SH)$ moieties are nearly planar rather than tetrahedral. In this model compound, the Si−OH_2 bond energy (35.9 kcal/mol) is somewhat larger than the Ge−OH_2 one (27.1 kcal/mol) by 8.8 kcal/mol. These results indicate that both the Si−OH and Si−OH_2 bond energies are much larger than the Ge−OH and Ge−OH_2 bond energies, respectively, and the difference between the Si−OH and Ge−OH bond energies is much larger than that between the Si−OH_2 and Ge−OH_2 bond energies. Hence, it is concluded that the conversion of the Si−OH bond to the Si−OH_2 is more difficult than that of the Ge−OH to the Ge−OH_2; in other words, the small reactivity of $\mathbf{1_{Si}}$ arises from the strong Si−OH bond. This is the reason why the Si element is not favorable for this process.

It is of importance to elucidate the reason why the Si−OH bond energy is much larger than the Ge−OH one. When two valence orbitals χ_A and χ_B form a covalent bond, its bond energy ΔE_{cov} is approximately represented by eq 1 based on the simple Hückel MO method;[47]

$$\Delta E_{cov} = \{(\varepsilon_A - \varepsilon_B)^2 + 4\beta^2\}^{1/2} \quad (1)$$

where ε_A represents the valence orbital energy of χ_A and β is a resonance integral between valence orbitals χ_A and χ_B. Because $\bullet SiPh_2(SH)$ radical has its valence orbital at a higher energy (−5.10 eV) than the $\bullet GePh_2(SH)$ one (−5.24 eV), the Si−OH bond energy is larger than the Ge−OH one; remember that the •OH radical has its valence orbital at a lower energy (−9.11 eV). In other words, the electropositive element more stabilizes the E−OH bond than the E−OH_2 one. Thereby, the too strong Si−OH bond is less reactive for the H−H σ-bond cleavage than the Ge−OH bond; see Figure S8 and the discussion below it for the Si−OH_2 and Ge−OH_2 bond energies.

Roles of the Ge Element in this Reaction. As mentioned above, the Ge element is crucial in this reversible reaction. In the H_2 coordination step, the μ-OH group dissociates from the Ru center to provide a coordination site for dihydrogen molecule. The Ge element assists this process by strengthening the Ge−OH bond. The Si element also plays the same role in this process. Because the activation energy of this step is smaller in the Si system than in the Ge one, it is suggested that the largely electropositive element is favorable for this process.

In the H−H σ-bond cleavage step, the Ge−OH/Si−OH bond is converted to the Ge−OH_2/Si−OH_2 bond. Because the Si−OH bond is too strong, the Si element is not favorable for this process; see above. It is noted here that the formation of the Ge−OH bond is crucial for the H−H σ-bond cleavage, because the Ge−OH moiety participates in the reaction. This is a newly found role of heavy main-group elements for σ-bond activation reactions.

The final step is the H_2O dissociation from the Ge/Si center. This process occurs with a similar activation energy for the Ge and Si systems. Considering these results, the use of a too strongly electropositive heavy main-group element is not

DOI: 10.1021/ic502463y
Inorg. Chem. 2015, 54, 576−585

recommended for this system. But, if a too weakly electropositive element is used, the first step becomes more difficult. Hence, the use of the Ge element is a reasonable choice.

CONCLUSIONS

The reversible reaction between H_2 and H_2O promoted by the hydroxo-/sulfido-bridged ruthenium−germanium dinuclear complex [Dmp(Dep)Ge(μ-S)(μ-OH)Ru(PPh_3)]$^+$ (**1**) (Dmp = 2,6-dimesitylphenyl, Dep = 2,6-diethylphenyl) was investigated with the ONIOM(B3LYP:UFF) method. In the H_2 conversion to H_2O, the first step is H_2 coordination with Ru, in which the Ru−O distance considerably increases to afford the intermediate **2** containing one vacant coordination site with activation energy of 14.3 (16.6) kcal/mol. Then, the H_2 further approaches the vacant site through the transition state $\mathbf{TS}_{2-3}$ with activation energy of 20.3 (25.1) kcal/mol to afford the dihydrogen σ-complex **3**. Starting from **3**, the H−H σ-bond cleavage by the Ru and Ge−OH moieties occurs with an activation energy of 11.6 (19.0) kcal/mol to form the intermediate **4**, in which hydride coordinates with the Ru center and H_2O interacts with the Ge center. The H−H σ-bond cleavage by the Ru and μ-S moieties needs a larger activation energy than that by the Ru and Ge−OH moieties. Finally, the H_2O dissociates from the Ge center with an activation energy of 23.5 (33.2) kcal/mol to afford [Dmp(Dep)Ge(μ-S)(μ-H)Ru(PPh_3)]$^+$ (**PRD**) and H_2O. This is the rate-determining step. The activation energy of the reverse reaction is 18.5 (26.7) kcal/mol. These values indicate that both the forward reaction of **1** with H_2 and the reverse reaction of **PRD** with H_2O occur with similar activation energies.

In the H−H σ-bond cleavage, the H^{α} atomic population moderately increases but the H^{β} atomic population considerably decreases when going to **4** from **3**, which indicates that this H−H σ-bond cleavage occurs in a heterolytic manner like hydrogenase.

In the Si analogue [Dmp(Dep)Si(μ-S)(μ-OH)Ru(PPh_3)]$^+$ ($\mathbf{1}_{Si}$), the H−H σ-bond cleavage becomes difficult. This is understood in terms of the E−O bond energy (E = Ge or Si); the Si−OH bond is too strong, and therefore, its conversion to the Si−OH_2 bond is not easy. This discussion suggests that the use of a more electropositive element than Ge is not recommended. But, if the less electropositive element is employed, the first step (**1** → **2**) providing the free E−OH moiety becomes difficult, suggesting that Ge is a good choice in this compound. One more important result here is that the Ge element plays crucial roles in σ-bond activation by providing the Ge−OH moiety which is reactive for the H−H σ-bond.

ASSOCIATED CONTENT

Supporting Information

Unabbreviated form of ref 34. Optimized geometries of **1** and this model complex with DFT(B3LYP) and ONIOM(B3LYP/BS1:UFF) methods (Table S1). Energy changes in H_2 coordination to Ru calculated with B3LYP/BS2 and ONIOM(B3LYP/BS2:UFF) (Table S2). Energy changes in path 1O calculated with the ONIOM(B3LYP/BS2:UFF), ONIOM(B3LYP-D3/BS2:UFF), and ONIOM(M06/BS2:UFF) methods (Table S3). The potential energy change with zero-point energy (E) in path 1O and the Gibbs energy (ΔG°) in paths 1O, 1S, 2S, 2O, and 1Si (Table S4, S5, S6, S7, and S8, respectively). Geometry changes in H_2 coordination to the μ-S side of **1** through path 2S (Figure S1). Geometry changes in H_2 coordination to [Dmp(Dep)Ge(μ-OH)(μ-S)Ru(PPh_3)]$^+$ (**1**) through path 2O (Figure S2). Energy changes in H_2 coordination to the Ru center on the μ-OH side through paths 1O, 1S, 2O, and 2S (Figure S3). Geometry changes in interconversion with [Dmp(Dep)Si(μ-OH)(μ-S)Ru(PPh_3)]$^+$ ($\mathbf{1}_{Si}$) (Figure S4). Geometry changes in interconversion using Real complex with B3LYP/BS2 (Figure S5). Energy changes in interconversion with ONIOM model **1**, the QM moiety of **1**, and Real complex **1** with DFT(B3LYP)/BS2//DFT(B3LYP)/BS1 (Figure S6). Cartesian coordinates of all species (Table S10). This material is available free of charge via the Internet at http://pubs.acs.org.

AUTHOR INFORMATION

Corresponding Authors

*(K.T.) E-mail: i45100a@nucc.cc.nagoya-u.ac.jp.

*(S.S.) E-mail: sakaki.shigeyoshi.47e@st.kyoto-u.ac.jp.

Present Addresses

‖Kyushu Sangyo University, 2-3-1 Matsukadai, Higashi-ku, Fukuoka 813-8503 Japan.

⊥Nippon Steel & Sumikin Chemical Co., Ltd., 46-80 Nakabaru Sakinohama, Tobata-ku, Kitakyushu 804-8503, Japan.

Notes

The authors declare no competing financial interest.

ACKNOWLEDGMENTS

This work is financially supported by the Ministry of Education, Culture, Science, Sport, and Technology through a Grant-in-Aid of Specially Promoted Science and Technology (No. 22000009, 23000007, and 23685015). We wish to thank the computer center of the Institute for Molecular Science (IMS, Okazaki, Japan) for kind use of computers.

REFERENCES

(1) (a) Kubas, G. J. *Comprehensive Organometallic Chemistry III* **2007**, *1*, 671. (b) Kubas, G. J. *Chem. Rev.* **2007**, *107*, 4152.

(2) Recent review: (a) Lubitzs, W.; van Gastel, M.; Gärtner, W. In *Metal Ions in Life Science*; Sigel, A., Sigel, H., Sigel, R. K. O., Eds.; John Wiley & son, Ltd: New York, 2006; Vol. 2, pp 279−158. (b) Evans, D. J.; Pickett, C. J. *Chem. Soc. Rev.* **2003**, *32*, 268. (c) Vignais, P. M.; Billoud, B. *Chem. Rev.* **2007**, *107*, 4206. (d) Fontecilla-Camps, J. C.; Volbeda, A.; Cavazza, C.; Nicolet, Y. *Chem. Rev.* **2007**, *107*, 4273. (e) De Lacey, A. L.; Fernández, V.; Rousset, M.; Cammack, R. *Chem. Rev.* **2007**, *107*, 4304. (f) Lubitz, W.; Reijerse, E.; van Gastel, M. *Chem. Rev.* **2007**, *107*, 4331. (g) Siegbahn, P. E. M.; Tye, J. W.; Hall, M. B. *Chem. Rev.* **2007**, *107*, 4414. (h) Ogata, H.; Lubitz, W.; Higuchi, Y. *Dalton Trans.* **2009**, 7577. (i) Lubitz, W.; Ogata, H.; Rüdiger, O.; Reijerse, E. *Chem. Rev.* **2014**, *114*, 4081.

(3) Nicolet, Y.; Lemon, B. J.; Fontecilla-Camps, J. C.; Peters, J. W. *Trends Biochem. Sci.* **2000**, *25*, 138.

(4) Peters, J. W. *Curr. Opin. Struct. Biol.* **1999**, *9*, 670.

(5) Przbyla, A. E.; Robbins, J.; Menon, N.; Peck, H. D., Jr. *FEMS Microbiol. Rev.* **1992**, *8*, 109.

(6) Garcin, E.; Vernede, X.; Hatchikian, E. C.; Volbeda, A.; Frey, M.; Fibtecilla-Camps, J. C. *Structure* **1999**, *7*, 557.

(7) Teixeira, M.; Moura, I.; Xavier, A. V.; Huynh, B. H.; DerVartanian, D. V.; Peck, H. D., Jr.; LeGall, J.; Moura, J. J. G. *J. Biol. Chem.* **1985**, *260*, 8942.

(8) Lyon, E. J.; Shima, S.; Boecher, R.; Thauer, R. K.; Grevels, F.-W.; Bill, E.; Roseboom, W.; Albracht, S. P. J. *J. Am. Chem. Soc.* **2004**, *126*, 14239.

(9) Shima, S.; Lyon, E. J.; Thauer, R. K.; Mienert, B.; Bill, E. *J. Am. Chem. Soc.* **2005**, *127*, 10430.

(10) Shima, S.; Pilak, O.; Vogt, S.; Schick, M.; Stagni, M. S.; Meyer-Klaucke, W.; Warjebtun, E.; Thauer, R. K.; Ermler, U. *Science* **2008**, *321*, 572.

DOI: 10.1021/ic502463y
Inorg. Chem. 2015, 54, 576−585

(11) Tard, C.; Pickett, C. J. *Chem. Rev.* **2009**, *109*, 2245.
(12) Linck, R. C.; Pafford, R. J.; Rauchfuss, T. B. *J. Am. Chem. Soc.* **2001**, *123*, 8856.
(13) Gray, T. G.; Veige, A. S.; Nocera, D. G. *J. Am. Chem. Soc.* **2004**, *126*, 9760.
(14) Bianchini, C.; Mealli, C.; Meli, A.; Sabat, M. *Inorg. Chem.* **1986**, *25*, 4617.
(15) (a) DuBois, M. R.; VanDerveer, M. C.; DuBois, D. L.; Haltiwanger, R. C.; Miller, W. K. *J. Am. Chem. Soc.* **1980**, *102*, 7456. (b) DuBois, M. R. *Chem. Rev.* **1989**, *89*, 1. (c) Laurie, J. C. V.; Duncan, L.; Haltiwanger, R. C.; Weberg, R. T.; DuBois, M. R. *J. Am. Chem. Soc.* **1986**, *108*, 6234.
(16) Kato, H.; Seino, H.; Mizobe, Y.; Hidai, M. *J. Chem. Soc., Dalton Trans.* **2002**, 1494.
(17) Ohki, Y.; Matsuura, N.; Marumoto, T.; Kawaguchi, H.; Tatsumi, K. *J. Am. Chem. Soc.* **2003**, *125*, 7978.
(18) (a) Ogo, S.; Kabe, R.; Uehara, K.; Kure, B.; Nishimura, T.; Menon, S. C.; Harada, R.; Fukuzumi, S.; Higuchi, Y.; Ohhara, T.; Tamada, T.; Kuroki, R. *Science* **2007**, *316*, 585. (b) Matsumoto, T.; Kure, B.; Ogo, S. *Chem. Lett.* **2008**, *37*, 970. (c) Wilson, A. D.; Shoemaker, R. K.; Miedaner, A.; Muckerman, J. T.; Dubois, D. L.; Dubois, R. M. *Proc. Natl. Acad. Sci. U.S.A.* **2007**, *104*, 6951. (d) Kure, B.; Matsumoto, T.; Ichikawa, K.; Fukuzumi, S.; Higuchi, Y.; Yagi, T.; Ogo, S. *Dalton Trans.* **2008**, 4747. (e) Matsumoto, T.; Kure, B.; Ogo, S. *Chem. Lett.* **2008**, *37*, 970.
(19) (a) Ogo, S.; Ichikawa, K.; Kishima, T.; Matsumoto, T.; Nakai, H.; Kusaka, K.; Ohhara, T. *Science* **2013**, *339*, 682. (b) Manor, B. C.; Rauchfuss, T. B. *J. Am. Chem. Soc.* **2013**, *135*, 11895.
(20) Matsumoto, T.; Nakaya, Y.; Itakura, N.; Tatsumi, K. *J. Am. Chem. Soc.* **2008**, *130*, 2458.
(21) Fulmer, G. R.; Muller, R. P.; Kemp, R. A.; Goldberg, K. I. *J. Am. Chem. Soc.* **2009**, *131*, 1346.
(22) (a) Trinquier, G.; Hoffmann, R. *Organometallics* **1984**, *3*, 370. (b) Ienco, A.; Calhorda, M. J.; Reinhold, J.; Reineri, F.; Bianchini, C.; Peruzzini, M.; Vizza, F.; Mealli, C. *J. Am. Chem. Soc.* **2004**, *126*, 11954.
(23) Gray, T. G.; Veige, A. S.; Nocera, D. G. *J. Am. Chem. Soc.* **2004**, *126*, 9760.
(24) (a) Maseras, F.; Morokuma, K. *J. Comput. Chem.* **1995**, *16*, 1170. (b) See recent review for instance, Chung, L. W.; Hirao, H.; Li, X.; Morokuma, K. *Comput. Mol. Sci.* **2011**, *2*, 327 and references therein.
(25) (a) Becke, A. D. *J. Chem. Phys.* **1983**, *98*, 5648. (b) Becke, A. D. *Phys. Rev.* **1988**, *A38*, 3098. (c) Lee, C.; Yang, W.; Parr, R. G. *Phys. Rev.* **1988**, *B37*, 785.
(26) (a) Miertus, S.; Scrocco, E.; Tomasi. *J. Chem. Phys.* **1981**, *55*, 117. (b) Pascual-Ahuir, J. L.; Silla, E.; Tomasi, J.; Bonaccorsi, R. *J. Comput. Chem.* **1987**, *8*, 778. (c) Floris, F.; Tomasi, J. *J. Comput. Chem.* **1989**, *10*, 616. (d) Tomasi, J.; Persico, M. *Chem. Rev.* **1994**, *94*, 2027.
(27) Andrae, D.; Haeussermann, U.; Dolg, M.; Stoll, H.; Preuss, H. *Theor. Chim. Acta* **1990**, *77*, 123.
(28) (a) Hehre, W. J.; Ditchfield, R.; Pople, J. A. *J. Chem. Phys.* **1972**, *56*, 2257. (b) Hariharan, P. C.; Pople, J. A. *Theor. Chim. Acta* **1973**, *28*, 213. (c) Hariharan, P. C.; Pople, J. A. *Mol. Phys.* **1974**, *27*, 209. (d) Francl, M. M.; Petro, W. J.; Hehre, W. J.; Binkley, J. S.; Gordon, M. S.; DeFrees, D. J.; Pople, J. A. *J. Chem. Phys.* **1982**, *77*, 3654.
(29) Martin, J. M. L.; Sundermann, A. *J. Chem. Phys.* **2001**, *114*, 3408.
(30) (a) Krishnan, R.; Binkley, J. S.; Seeger, R.; Pople, J. A. *J. Chem. Phys.* **1980**, *72*, 650. (b) McLean, A. D.; Chandler, G. S. *J. Chem. Phys.* **1980**, *72*, 5639. (c) Blaudeau, J.-P.; McGrath, M. P.; Curtiss, L. A.; Radom, L. *J. Chem. Phys.* **1997**, *107*, 5016. (d) Curtiss, L. A.; McGrath, M. P.; Blandeau, J.-P.; Davis, N. E.; Binning, R. C.; Radom, L., Jr. *J. Chem. Phys.* **1995**, *103*, 6104.
(31) Clark, T.; Chandrasekhar, J.; Spitznagel, G. W.; Schleyer, P. V. R. *J. Comput. Chem.* **1983**, *4*, 294.
(32) Mammen, M.; Shakhnovich, E. I.; Deutch, J. M.; Whitesides, G. M. *J. Org. Chem.* **1998**, *63*, 3821−3830.
(33) (a) Ishikawa, A.; Nakao, Y.; Sato, H.; Sakaki, S. *Inorg. Chem.* **2009**, *48*, 8154−8163. (b) Zeng, G.; Sakaki, S. *Inorg. Chem.* **2011**, *50*, 5290−5297. (c) Zeng, G.; Sakaki, S. *Inorg. Chem.* **2012**, *51*, 4597−4605. (d) Aono, S.; Sakaki, S. *J. Phys. Chem. B* **2012**, *116*, 13045−13062.
(34) Pople, J. A., et al. *Gaussian 03*, revision C.02; Gaussian, Inc.: Wallingford, CT, 2004.
(35) Reed, A. E.; Curtiss, L. A.; Weinhold, F. *Chem. Rev.* **1988**, *88*, 899.
(36) We expected that H_2 coordination occurs concomitantly with the Ru−O bond lengthening. We tried to find such a transition state but failed. This is not surprising because the six-coordinating Ru center is saturated and any ligand cannot approach the Ru center without dissociation of one ligand.
(37) Experimental and experiment−computation joint studies: (a) Peris, E.; Lee, J. C.; Rambo, J. R.; Eisenstein, O.; Crabtree, R. H. *J. Am. Chem. Soc.* **1995**, *117*, 3485. (b) Wessel, J.; Lee, J. C.; Peris, E.; Yap, G. P. A.; Fortin, J. B.; Ricci, J. S.; Sini, G.; Albinati, A.; Koetzle, T. F.; Eisenstein, O.; Rheingold, A. L.; Crabtree, R. H. *Angew. Chem., Int. Ed. Engl.* **1995**, *34*, 2507. (c) Belkova, N. V.; Epstein, L. M.; Shubina, E. S. *Eur. J. Inorg. Chem.* **2010**, *2010*, 3555. (d) Basallote, M. G.; Besora, M.; Castillo, C. E.; Fernández-Trujillo, M. J.; Lledós, A.; Maseras, F.; Máñez, M. A. *J. Am. Chem. Soc.* **2007**, *129*, 6608. (e) Belkova, N. V.; Shubina, E. S.; Epstein, L. M. *Acc. Chem. Res.* **2005**, *38*, 624. (f) Liu, T.; Wang, X.; Hoffmann, C.; DuBois, D. L.; Bullock, R. M. *Angew. Chem., Int. Ed. Engl.* **2014**, *53*, 5300. Theoretical studies: (g) Liu, Q.; Hoffmann, R. *J. Am. Chem. Soc.* **1995**, *117*, 10108. (h) Orlova, G.; Scheiner, S. *J. Phys. Chem. A* **1998**, *102*, 260.
(38) (a) Cygan, Z. T.; Kampf, J. W.; Holl, M. M. B. *Inorg. Chem.* **2003**, *42*, 7219. (b) Kubas, G. J. *Metal Dihydrogen and sigma-Bond Complexes: Structure, Theory, and Reactivity*; Kluwer Academic/Plenum Publishers: New York, 2005.
(39) The number without parenthesis means the potential energy change with zero-point energy correction. The number in parenthesis means the Gibbs energy change.
(40) Since adduct **2** is formed from **1** and H_2, it is likely that the potential energy change is considerably different from the Gibbs energy change. However, the difference is not large (0.6 kcal/mol). Because the H_2 weakly coordinates to the Ru center in $\mathbf{TS}_{1-2}$ and **2**, vibration motions between H_2 and the Ru center occur with low frequencies. These low frequencies contribute to the large partition function and hence the large entropy. As a result, the Gibbs energy does not increase very much compared to the increase in potential energy.
(41) Zhao, Y.; G. Truhlar, D. *Theor. Chem. Acc.* **2008**, *120*, 215.
(42) For instance: (a) Siegbahn, P. E. M. *Adv. Inorg. Chem.* **2004**, *56*, 101. (b) Cao, Z.; Hall, M. B. *J. Am. Chem. Soc.* **2001**, *123*, 7877. (c) Ref 2g and references therein..
(43) Vincent, J. L.; Luo, S.; Scott, B. L.; Butcher, R.; Unkefer, C. J.; Burns, C. J.; Kubas, G. J.; Lledós, A.; Maseras, F.; Tomàs, J. *Organometallics* **2003**, *22*, 5307.
(44) (a) Biswas, B.; Sugimoto, M.; Sakaki, S. *Organometallics* **2000**, *19*, 3895. (b) Musashi, Y.; Sakaki, S. *J. Am. Chem. Soc.* **2000**, *122*, 3867. (c) Ochi, N.; Nakao, Y.; Sato, H.; Sakaki, S. *J. Am. Chem. Soc.* **2007**, *129*, 8615. (d) Ochi, N.; Nakao, Y.; Sato, H.; Sakaki, S. *Can. J. Chem.* **2009**, *87*, 1415. (e) Sakaki, S.; Sato, H.; Ohnishi, Y.-y. *Chem. Rec.* **2010**, *10*, 29. (f) Guan, W.; Sayyed, F. B.; Zeng, G.; Sakaki, S. *Inorg. Chem.* **2014**, *53*, 6444.
(45) For instance: (a) Welch, G. C.; San Juan, R. R.; Masuda, J. D.; Stephan, D. W. *Science* **2006**, *314*, 1124. (b) Stephan, D. W. *Dalton Trans.* **2009**, 3129.
(46) (a) Rokob, T. A.; Hamza, A.; Stiring, A.; Soòs, T.; Pápai, I. *Angew. Chem., Int. Ed.* **2008**, *47*, 2435. (b) Holschumacher, D.; Bannenberg, T.; Hrib, C. G.; Jones, P. G.; Tamm, M. *Angew. Chem., Int. Ed.* **2008**, *47*, 7428.
(47) (a) Biswas, B.; Sugimoto, M.; Sakaki, S. *Organometallics* **1998**, *17*, 1278. (b) Sakaki, S.; Kai, S.; Sugimoto, M. *Organometallics* **1999**, *18*, 4825. (c) Biswas, B.; Sugimoto, M.; Sakaki, S. *Organometallics* **1999**, *18*, 4015. (d) Sumimoto, M.; Iwane, N.; Takahama, T.; Sakaki, S. *J. Am. Chem. Soc.* **2004**, *126*, 10457. (e) Ray, M.; Nakao, Y.; Sato, H.; Sakaba, H.; Sakaki, S. *Organometallics* **2009**, *28*, 65. (f) Sugiyama,

DOI: 10.1021/ic502463y
Inorg. Chem. 2015, 54, 576−585

A.; Ohnishi, Y.-y.; Nakaoka, M.; Nakao, Y.; Sato, H.; Sakaki, S.; Nakao, Y.; Hiyama, T. *J. Am. Chem. Soc.* **2008**, *130*, 12975.

DOI: 10.1021/ic502463y
Inorg. Chem. 2015, 54, 576−585